

Density and magnetic field gradients in Tycho SNR

Introduction

- Remnant of SN1572, size 8', distance 2.3 kpc
- Expansion into inhomogeneous ISM [1, 2]
- Interaction with dense clouds on East and NW [3, 4]
- Presence of a large scale density gradient [5, 6]
- **What is the direction of the density gradient?**
- **What about the magnetic field distribution?**

Utilizing the pixel-to-pixel analysis of the radio and X-ray images of Tycho SNR as well as theoretical properties of emission, we obtained the images for the post-shock density and magnetic field strength over the remnant.

By using these maps, we further derived the spatial distributions of both the cut-off frequency and the maximum energy of electrons and commented on gamma-ray emission from Tycho SNR.

Observations

- VLA radio map (q_r), 2014, 1.4 GHz, resolution 1.91'' [2]
- LOFAR radio index map (α), 2013-2016, 48-1400 MHz, resolution 40'' [7]
- Chandra X-ray map (q_x), 2015, 1.2-4.0 keV, resolution 0.492''
- Chandra X-ray map (q_{xs}), 2015, 4.0-6.0 keV, resolution 0.492''
- All images were reprojected to the same pixel grid to allow for the pixel-to-pixel analysis.

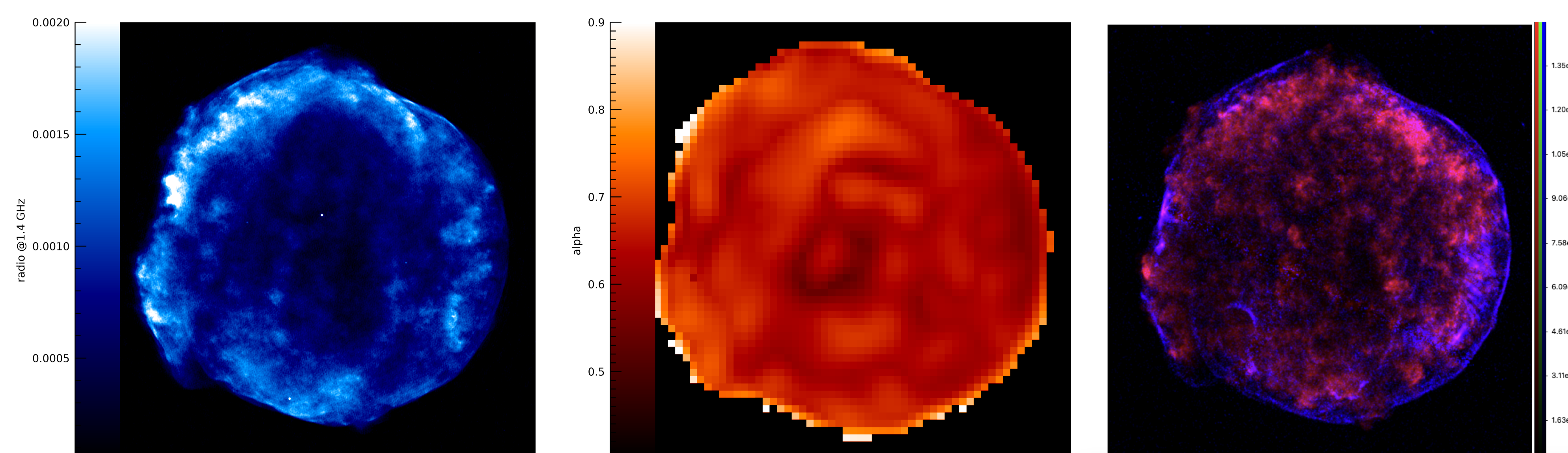


Figure 1: Radio (left), radio index (center) and X-ray (right) images of Tycho SNR. X-ray colors: 1.2-4.0 keV (red), 4.1-6.0 keV (blue).

Gradients of density n and magnetic field strength B

- Radio $q_r \propto \eta_r n B^{\alpha+1}$
- Thermal X-ray $q_x \propto \eta_x n^2 \Lambda$
- Band where $\Lambda(T, \tau) \approx \text{const}$
- Geometric factors η_r, η_x account for the internal structure along LoS
- $n \propto \left(\frac{q_x}{\eta_x}\right)^{1/2}$
- $B \propto \left(\frac{q_r^2 \eta_x}{q_x \eta_r^2}\right)^{1/(2\alpha+2)}$

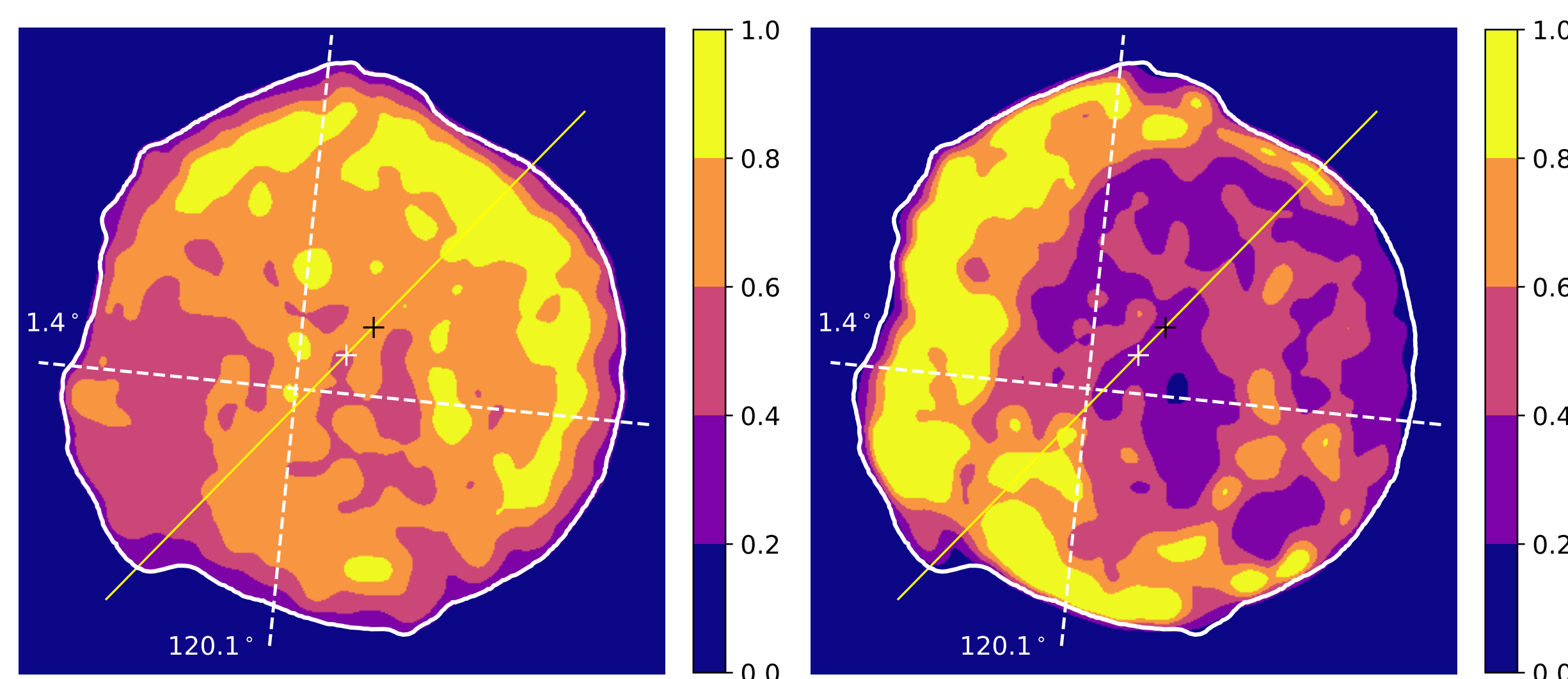


Figure 2: Maps of n (left) and B (right). Geometric center (white cross) and explosion site (black cross) are also shown.

Conclusions: gradients

- Density gradient is in the North-West direction.
- Yellow line passes through the two centers. Coincides with $\text{grad}(n)$. Independent confirmation of the explosion location.
- Density enhancements pre-shock at East and NW [1, 6]. Our results: a large scale $\text{grad}(n)$ is toward NW, while the shock hit a local overdensity at East just recently.
- Gradient of magnetic field strength points toward the East.
- $\text{grad}(B)$ is parallel to the Galactic plane.

Cut-off frequency ν_{cr} and maximum energy E_{max} of electrons

- B on Fig. 2 is in arbitrary units. Convert to physical: set $\langle B \rangle = 120 \mu\text{G}$. This provides $B \approx 200 \mu\text{G}$ around the rim [8].
- Cut-off frequency ν_{cr} for electrons with energy E_{max} is calculated by fitting, for each pixel, the synchrotron spectrum from radio (q_r) to X-rays (q_{xs}) and assuming the electron momentum distribution as a power-law (α) with an exponential cut-off.
- $E_{\text{max}} = \left(\frac{\nu_{\text{cr}}}{c_1 B}\right)^{1/2}$

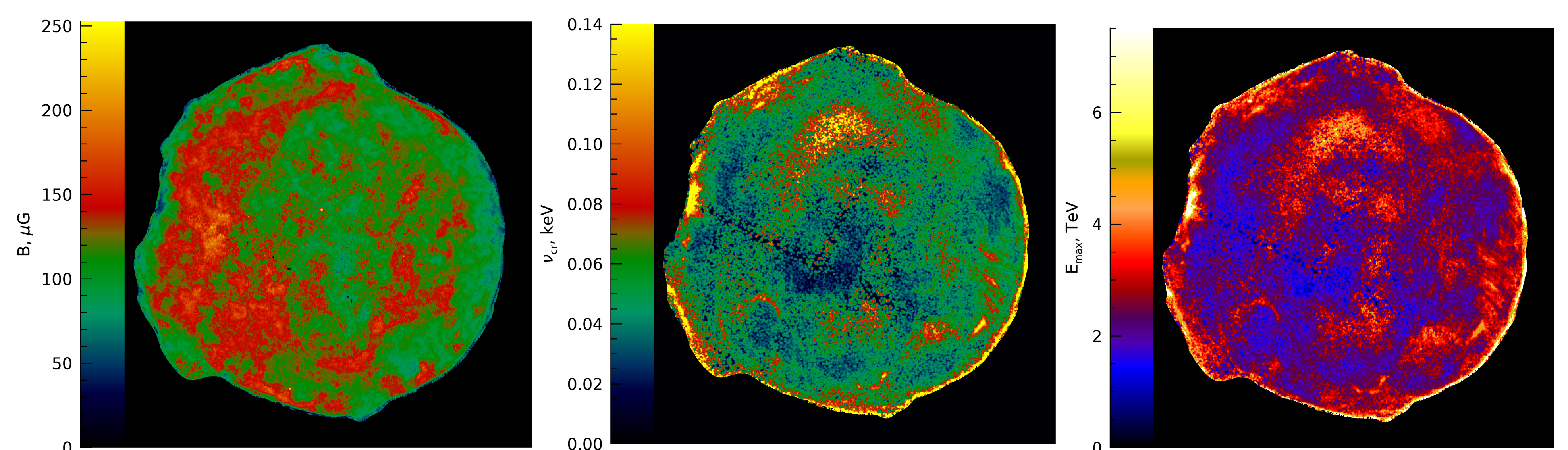


Figure 3: Maps of B (left), cut-off energy ν_{cr} (center), maximum energy of electrons E_{max} (right)

Conclusions: E_{max}

- X-ray emitting electrons lose energy quickly \Rightarrow thin rims for ν_{cr} and E_{max} .
- E_{max} is in the range 5 – 7 TeV around the rim. This is in agreement with [9].
- $E_{\text{max}} \simeq 11$ TeV is greatest at East where the shock encountered the local overdensity recently.
- Higher E_{max} also around the stripes at West and the arch at South-East.

Discussion: γ -rays

- GeV and TeV γ -rays are detected from Tycho SNR [10, 11].
- Two preferable locations for γ -rays, with enhanced ambient density: @East, @NW
- The shock speed $V \approx 2000$ and 3400 km/s at East and NW. Efficient acceleration and γ -rays @NW?
- Our analysis: East is preferable (V has decreased recently, E_{max} is the highest).

References

1. Reynoso et al. 1997 ApJ, 491, 816
2. Williams et al. 2016 ApJL, 823, L32
3. Lee et al. 2004 ApJL, 605, L113
4. Chen et al. 2017 A&A, 604, A13
5. Vigh et al. 2011 ApJ, 727, 32
6. Williams et al. 2013 ApJ, 770, 129
7. Arias et al. 2019 AJ, 158, 253
8. Reynolds et al. 2021 ApJ, 917, 55
9. Parizot et al. 2006 A&A, 453, 387
10. Giordano et al. 2012 ApJL, 744, L2
11. Acciari et al. 2011 ApJL, 730, L20